Cold-regions river flow observed from space

A. Kääb[1] and T. Prowse[2]

Received 4 February 2011; revised 7 March 2011; accepted 9 March 2011; published 20 April 2011.

[1] Knowledge of water-surface velocities in rivers is useful for understanding a wide range of lotic processes and systems, such as water and ice fluxes and forces, mixing, solute and sediment transport, bed and bank stability, aquatic and riparian ecology, and extreme hydrologic events. In cold regions, river-ice break up and the associated downstream transport of ice debris is often the most important hydrological event of the year, producing flood levels that commonly exceed those for the open-water period and dramatic consequences for river infrastructure and ecology. Quantification of river surface velocity and currents has relied mostly on very scarce *in situ* measurements or particle tracking in laboratory models, with few attempts to cover entire river reaches. Accurate and complete surface-velocity fields on rivers have rarely been produced. Here, we use river-ice debris as an index of surface water velocity, and track it over a time period of about one minute, which is the typical time lapse between the two or more images that form a stereo data set in spaceborne, alongtrack optical-stereo mapping. In this way, we measure and visualize for the first time, the almost complete surface velocity field of a river. Examples are used from approximately 80 km and 40 km long reaches of the St. Lawrence and Mackenzie rivers, respectively. The methodology and results will be valuable to a number of disciplines requiring detailed information about river flow, such as hydraulics, hydrology, river ecology and natural-hazard management. **Citation:** Kääb, A., and T. Prowse (2011), Cold-regions river flow observed from space, *Geophys. Res. Lett.*, *38*, L08403, doi:10.1029/2011GL047022.

1. Introduction

[2] Scientific and applied studies have attempted for decades to quantify complete surface-velocity fields on rivers but with limited success. The high level of interest in obtaining such information is because velocity-controlled water fluxes and forces lead to the erosion, transport and deposition of material in river channels and along their banks, with important implications for river ecology, fluvial geomorphology and human infrastructure. Engineering of in-channel and bank-side installations, for example, requires estimation of water discharge, forces and sediment erosion/transport. In cold regions, such needs are magnified by the complicating effects of river ice, the break-up of which often creates the most important hydrological event of the year [*Prowse*, 2005]. Even estimating discharge during this period and, for instance, the associated freshwater fluxes into the Arctic and circum-Arctic Oceans [*Peterson et al.*, 2002], however, is notoriously difficult and often inaccurate due to the ice disruption of hydrometric equipment and effects on stage-discharge rating curves [*Shiklomanov et al.*, 2006; *White and Beltaos*, 2008]. Break-up can also severely affect river ecosystems and human infrastructure, such as settlements, bridges and hydro-electric facilities [*Gerard and Davar*, 1995; *Prowse and Culp*, 2003]. Of particular importance are ice-jam-generated waves (or javes) that can travel rapidly downstream and be especially destructive [*Jasek and Beltaos*, 2008]. The economic costs from break-up ice jams are estimated to average almost 250 million USD per year in North America and to have been over 100 million USD for a single 2001-event in Eastern Russia [*Prowse et al.*, 2007]. Although typically less dynamic than break-up, freeze-up can create a similar array of bio-geophysical problems on many cold-regions rivers. Overall, the monitoring, field study and modelling of river conditions during these two periods has been hampered by a lack of comprehensive water and ice velocity fields.

[3] Remote sensing offers a possibility to obtain such information. Previous relevant studies investigated, for example: subtle river-ice deformation using radar interferometry [*Smith*, 2002; *Vincent et al.*, 2004]; ocean currents from repeat spaceborne optical, thermal or microwave imagery, such as by tracking sea-ice or sea-surface temperature features [*Lavergne et al.*, 2010; *Matthews and Emery*, 2009]; river-ice properties and density from radar imagery [*Mermoz et al.*, 2009; *Unterschultz et al.*, 2009]; flow velocities from suspended-sediment concentrations in optical satellite images [*Pavelsky and Smith*, 2009]; river-ice temperatures [*Emond et al.*, 2011]; surface water flow from tracking foam or ice debris in ground-based or laboratory video-image sequences using particle image velocimetry techniques [*Creutin et al.*, 2003; *Ettema et al.*, 1997; *Jasek et al.*, 2001]. River and ocean currents have in particular been derived using spaceborne and airborne alongtrack radar interferometry [*Goldstein and Zebker*, 1987; *Graber et al.*, 1996; *Siegmund et al.*, 2004; *Romeiser et al.*, 2007, 2010]. The time interval or the related angular difference between alongtrack stereo imagery, originally designed to map terrain topography, have so far been little exploited for water applications, but have been used to derive vehicle and wave speeds and ocean currents [*Garay and Diner*, 2007; *Matthews*, 2005; *Matthews and Awaji*, 2010].

2. Data and Method

[4] Our methodology consists of two key elements. Firstly, we use ice debris associated with river-ice break up as an index for surface-water velocities. This is based on the assumption that the ice-debris velocity is similar to that of the water velocity, although this could vary slightly

[1]Department of Geosciences, University of Oslo, Oslo, Norway.
[2]Water and Climate Impacts Research Centre, Environment Canada, University of Victoria, Victoria, British Columbia, Canada.

0094-8276/11/2011GL047022

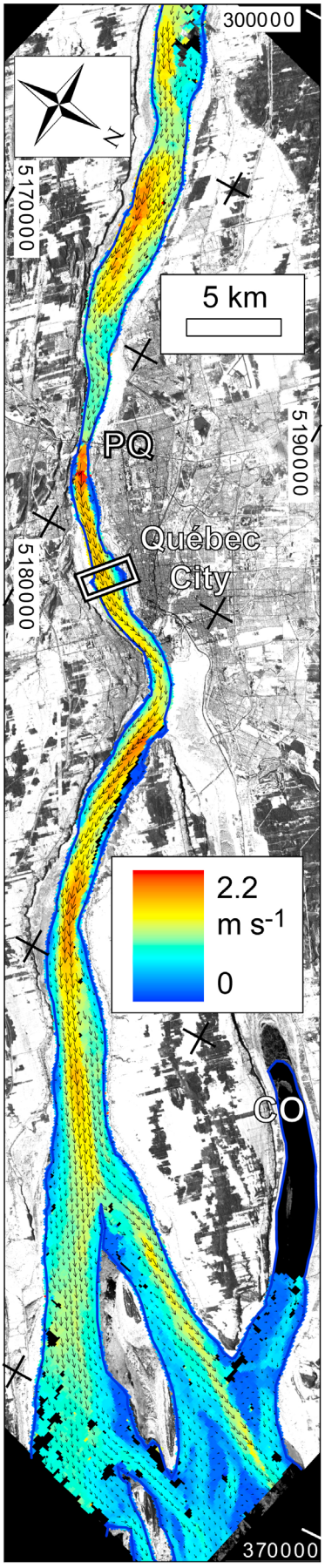

depending on frictional drag as partly influenced by the submerged depth of the ice or wind effects on its exposed surface. Such ice debris is visible in high and medium resolution satellite images acquired during a certain time period after ice break-up. Secondly, we exploit the fact that the two or more images forming along-track stereo data from a moving airborne or spaceborne platform are acquired with a temporal separation, which is basically defined by the sensor travel speed above ground, and the base-to-height ratio of the system. For our two study sites in Canada, we apply: a satellite stereo image pair from the Advanced Spaceborne Thermal Emission and Reflection Radiometer (ASTER) on board the NASA Terra spacecraft with 15 m ground resolution and 55.3 s time lapse; a triplet stereo scene from the Panchromatic Remote-sensing Instrument for Stereo Mapping (PRISM) on board the Japanese ALOS satellite with 2.5 m ground resolution and 45 s or 90 s, respectively, time lapse; and an IKONOS satellite stereo pair of 1 m ground resolution and ~53 s time lapse. The stereo images are co-registered using a first-order polynomial transformation based on automatically matched (see below) stable objects at surface water level along the river margins. Ice debris is then tracked between two images with sub-pixel precision by maximizing the double normalized cross-correlation coefficient on a regular grid of small image templates [*Kääb and Vollmer*, 2000]. Erroneous measurements are filtered out by a threshold on the correlation coefficient and a 3 × 3 moving window median filter. The resulting displacements are converted to velocity using the time interval between the stereo images.

3. Results

[5] We demonstrate river-velocity fields for two different types of river morphologies and the above three different spaceborne stereo sensors. Surface velocities on the St. Lawrence River at its mouth near Québec City (46.8°N, 71.2°W) are measured along a ~80 km long river reach obtained from an ASTER stereo pair of 30 January 2003 (Figure 1). This reach is influenced by tides with a mean water level of 2.3 [2.7] m asl. and a mean tidal range of 2.1 [4.9] m (2.8 [6.4] m for large tides) at the up-stream [downstream] end. Depending on the tide propagation, the total elevation difference over the 80 km is only a maximum of a few meters and, therefore, topographic distortions in the stereo data can be neglected for the river surface. Velocities are derived using image templates of 9 × 9 pixels in size (135 m × 135 m) over a 100 m grid spacing resulting in

Figure 1. Colour-coded surface flow velocities and vectors on the St. Lawrence River at Québec City, Canada, from an ASTER satellite stereo pair of 30 January 2003 (background) acquired at around 15:50 UTC. The blue outline indicates the boundary of open water. Black data voids in the river and on the entire river branch to the middle right (Chenal de l' Ile d' Orleans; CO) indicate open water without trackable ice debris. For better visibility, the velocity vectors, originally measured with 100 m spacing, have been resampled to 400 m spacing. The white rectangle at Québec City shows the position of Figure 2. PQ, Pont de Québec bridge. Coordinate grid UTM zone 19.

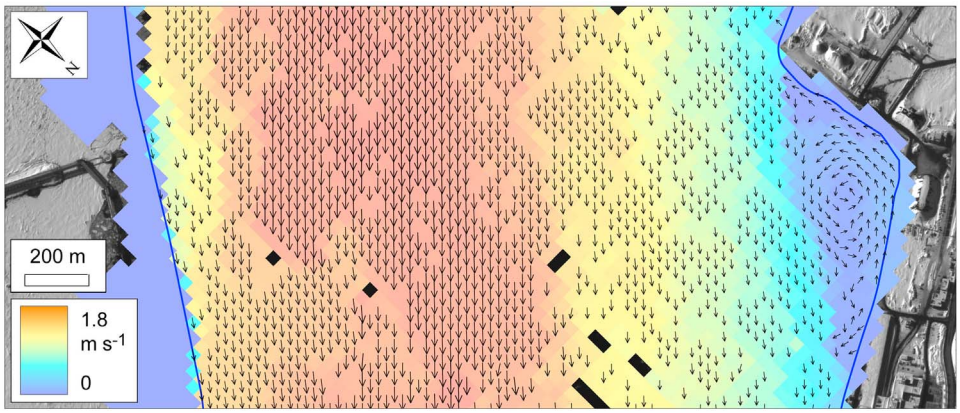

Figure 2. Surface flow velocities and vectors on the St. Lawrence River at Québec City, derived from an IKONOS satellite stereo pair (background) of 19 February 2000 at around 15:19 UTC. The blue outline indicates the boundary of open water. Black data voids in the river indicate open water without ice debris tracked. All successfully measured velocity vectors are show (25 m spacing). The underlying IKONOS image is copyright GeoEye. Image centre lat/lon is ~46.787°N/71.217°W. For image location see also Figure 1.

~20,000 measurements after outlier filtering. In general, the ice floes are unconnected and are thus assumed to reflect uninterrupted surface flow. This is not the case, however, for a ~6 km section upstream of the narrows at the Québec City bridge (PQ in Figure 1) where an ice accumulation exists. Here, ice floes are juxtaposed in the flow with velocities of only ~0.9 m s^{-1} at mid-channel. About 1.5 km downstream from this site, maximum mid-channel floe velocities increase to 2.2 m s^{-1}. Based on image correlation results for stranded, i.e., non-moving ice debris and fast ice along the banks, we estimate an overall accuracy of ~0.25 pixels (3.8 m, 0.07 m s^{-1}) for the velocities from the ASTER data. In general, the effect of varying channel width and direction are reflected in the derived flow speeds and vectors, respectively.

[6] For a ~13 km sub-reach in the above ASTER scene, 1 m resolution IKONOS stereo data were acquired on 19 February 2000 (Figure 2). About 10,000 valid matches are obtained using 25 × 25 pixel sized templates (25 m × 25 m) over a 25 m regular grid. Again, the displacements of the unconnected ice floes and debris over the observation period are assumed to represent surface water velocities. In this case, comparison to stationary ice along the banks indicates an overall accuracy of ~0.7 pixels (0.7 m, 0.01 m s^{-1}). The IKONOS-derived mid-channel surface velocities of February 2000 are up to 18 % higher than those derived from ASTER for January 2003, a difference not unreasonable over such an interval. Towards the river banks, percentage differences are partly larger due to different water levels and fast ice remnants between the two observation dates. Of particular note in the image is the backwater eddy characterized by a reversal of flow in the embayment along the left bank (right side of image). The low velocities along this bank contrast strongly with the uninterrupted higher-velocity flow along the mid-channel.

[7] To investigate a river morphology very different from the St. Lawrence River at its mouth, surface velocities on a 40 km long, high-latitude, main-stem reach of the Mackenzie River (67.3°N, 130.8°W) are measured (Figure 3). In contrast to the relatively straight reach of the St. Lawrence, the one selected for the Mackenzie River is braided and meandering with sand bars. An ALOS PRISM stereo triplet of 21 May 2008 is used with 45 s time separation between the forward and nadir as well as the nadir and backward looking data, and 90 s between the forward and backward data, respectively. The water level at this section is ~15 m asl. with a relatively low slope making topographic distortions on the water surface negligible. Surface velocities are measured with 40 × 40 pixel sized templates (100 m × 100 m) over a 75 m grid resulting in ~13,000 measurements. Again, widely distributed and unconnected ice floes and debris ensure that their displacements over the observation period are representative of surface water velocities. Accuracy in this case, based on reference measurements to stationary shore ice, is ~0.5 pixels (1.3 m, 0.03 m s^{-1}). To investigate the potential influence of shallow bed sections in this reach on ice motion and velocities, small island and sand-bar locations are identified from additional satellite images (ALOS AVNIR, 1 October 2006; Landsat5 path 60/row 13, 21 June 2008; Landsat7 path 60/row 13, 1 October 2007). In general, high flow and water-level conditions on 21 May 2008 (as indicated by the Arctic Red River hydrometric station, 10LC014, located 140 km downstream) suggest maximum inundation of any sand bars. The location of bars and islands is obtained during periods of relatively low flow (near annual minima) from satellite imagery of 1 October 2006 (ALOS AVNIR) and cross-checked with other images for 1 October 2007 and 21 June 2008 (Landsat5 and 7) to ensure that river morphology remained stable between October 2006 and May 2008. Zones inundated in the May 2008 images but not in those of October 2006 are used as indicators of more shallow water. (The water level difference at the 10LC014 station between end May 2008 and October 2008, for instance, is approximately 8 m.) Despite being in central channel locations, flow velocities over these locations are relatively slow, sometimes reaching as low as 0.5 to 1 m s^{-1}. By contrast, maximum surface velocities are slightly over 3 m s^{-1} at the narrowest river section where

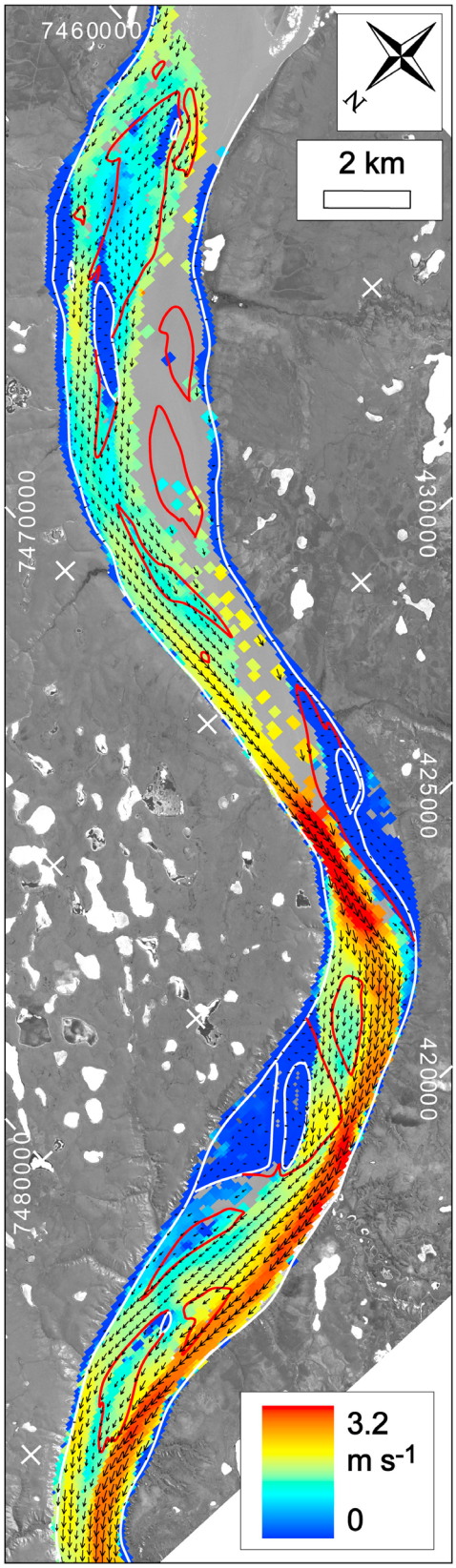

the flow is concentrated and velocities should be greatest. Both of these examples reflect the ability of the technique to map spatial differences in velocity fields resulting from variations in channel depth and width.

4. Conclusions

[8] Based on the success of this study, it is now possible to derive measurement of two-dimensional river-surface velocity fields over entire river reaches, which creates a wide range of new opportunities for geophysical, ecological and engineering applications. This testing of the technique was possible only because of the fortuitous availability of archived satellite records, which currently contain very limited and short intervals of relevant data for river freeze-up and break-up periods. For future applications, however, acquisition plans of existing and upcoming airborne and spaceborne missions could be modified to target selected rivers around freeze-up and break-up periods, thereby greatly enhancing the applicability of the method. As for all optical space-based methods, however, this new method is restricted for use with cloud-free day-time data, a particular limitation for high latitudes. Although ice-velocity information alone would be highly valuable for many applications, the additional application of hydraulic formula to account for variations in velocity with flow depth would also permit the estimation of discharge during these key times on remote high-latitude rivers. Deriving more accurate estimates of such northern flows would be invaluable, for example, to improving our understanding of the freshwater budget of the Arctic Ocean, which is known to have important implications for global climate. Although the demonstrated approach relies on ice debris as surface markers means it is restricted to cold region rivers and over specific periods (freeze-up and break-up), other potential tracers, such as drifting matter, sediment plumes or thermal variations, could expand its application to other regions.

[9] **Acknowledgments.** This study was supported by The Research Council of Norway (NFR) through the CORRIA project (185906/V30) and the International Centre for Geohazards (SFF-ICG 146035/420), and the National Sciences and Engineering Research Council of Canada, Environment Canada, and the International Polar Year program. It is a contribution to the 'Monitoring Earth surface changes from space' study by the Keck Institute for Space Studies at Caltech/JPL. ASTER data are courtesy of NASA/GSFC/METI/ERSDAC/JAROS, and the US/Japan ASTER science team, and were obtained within the Global Land Ice Measurements from Space project. ALOS PRISM and AVNIR data are courtesy of AOALO.3579, copyright ESA; IKONOS data are copyright GeoEye Inc. Topographic data are courtesy of the Canadian GeoBase initiative,

Figure 3. Surface flow velocities and vectors on the Mackenzie River, Canadian Arctic, derived from an ALOS PRISM satellite stereo triplet of 21 May 2008 acquired at around 20:30 UTC. The red outlines indicate sand bars visible at low water level, the white lines vegetated islands and river margins assumed to be not or only slightly flooded during high water. Grey data voids in the river indicate open water without ice debris tracked. For better visibility, the velocity vectors with 75 m original spacing have been resampled to 225 m spacing. Image centre lat/lon is ~67.33°N/130.70°W. Coordinate grid UTM zone 9.

tidal data of Fisheries and Oceans Canada (Canadian Hydrographic Service), and hydrological data of Environment Canada (Water Survey). The authors thank Tamlin Pavelsky and an anonymous reviewer for their assistance in evaluating this paper.

[10] The Editor thanks Tamlin Pavelsky and an anonymous reviewer for their assistance in evaluating this paper.

References

Creutin, J. D., M. Muste, A. A. Bradley, S. C. Kim, and A. Kruger (2003), River gauging using PIV techniques: A proof of concept experiment on the Iowa River, *J. Hydrol.*, *277*(3–4), 182–194.

Emond, J., B. Morse, M. Richard, E. Stander, and A. A. Viau (2011), Surface ice observations on the St. Lawrence River using infrared thermography, *River Res. Appl.*, doi:10.1002/rra.1445, in press.

Ettema, R., I. Fujita, M. Muste, and A. Kruger (1997), Particle-image velocimetry for whole-field measurement of ice velocities, *Cold Reg. Sci. Technol.*, *26*(2), 97–112.

Garay, M. J., and D. J. Diner (2007), Multi-angle Imaging SpectroRadiometer (MISR) time-lapse imagery of tsunami waves from the 26 December 2004 Sumatra-Andaman earthquake. *Remote Sens. Environ.*, *107*(1–2), 256–263.

Gerard, R. L., and K. S. Davar (1995), Introduction, in *River Ice Jams*, edited by S. Beltaos, pp. 1–28, Water Resour., Highlands Ranch, Colo.

Goldstein, R. M., and H. A. Zebker (1987), Interferometric radar measurement of ocean surface currents, *Nature*, *328*(6132), 707–709.

Graber, H. C, D. R. Thompson, and R. E. Carande (1996), Ocean surface features and currents measured with synthetic aperture radar interferometry and HF radar, *J. Geophys. Res.*, *101*(C11), 25813–25832.

Jasek, M., and S. Beltaos (2008), Ice-jam release: Javes, ice runs and breaking fronts, in *River Ice Breakup*, edited by S. Beltaos, pp. 247–303, Water Resour., Highlands Ranch, Colo.

Jasek, M., M. Muste, and R. Ettema (2001), Estimation of Yukon River discharge during an ice jam near Dawson City, *Can. J. Civ. Eng.*, *28*, 856–864.

Kääb, A., and M. Vollmer (2000), Surface geometry, thickness changes and flow fields on creeping mountain permafrost: Automatic extraction by digital image analysis, *Permafrost Periglacial Processes*, *11*(4), 315–326.

Lavergne, T., S. Eastwood, Z. Teffah, H. Schyberg, and L.-A. Breivik (2010), Sea ice motion from low-resolution satellite sensors: An alternative method and its validation in the Arctic, *J. Geophys. Res.*, *115*, C10032, doi:10.1029/2009JC005958.

Matthews, D. K., and W. J. Emery (2009), Velocity observations of the California Current derived from satellite imagery, *J. Geophys. Res.*, *114*, C08001, doi:10.1029/2008JC005029.

Matthews, J. (2005), Stereo observation of lakes and coastal zones using ASTER imagery, *Remote Sens. Environ.*, *99*(1–2), 16–30.

Matthews, J. P., and T. Awaji (2010), Synoptic mapping of internal-wave motions and surface currents near the Lombok Strait using the Along-Track Stereo Sun Glitter technique, *Remote Sens. Environ.*, *114*(8), 1765–1776.

Mermoz, S., S. Allain, M. Bernier, E. Pottier, and I. Gherboudj (2009), Classification of river ice using polarimetric SAR data, *Can. J. Remote Sens.*, *35*(5), 460–473.

Pavelsky, T. M., and L. C. Smith (2009), Remote sensing of suspended sediment concentration, flow velocity, and lake recharge in the Peace-Athabasca Delta, Canada, *Water Resour. Res.*, *45*, W11417, doi:10.1029/2008WR007424.

Peterson, B. J., R. M. Holmes, J. W. McClelland, C. J. Vörösmarty, R. B. Lammers, A. I. Shiklomanov, I. A. Shiklomanov, and S. Rahmstorf (2002), Increasing river discharge to the Arctic Ocean, *Science*, *298* (5601), 2171–2173.

Prowse, T. D. (2005), River-ice hydrology, in *Encyclopedia of Hydrological Sciences*, edited by M. G. Anderson, pp. 648–650, John Wiley, West Sussex, U. K.

Prowse, T. D., and J. M. Culp (2003), Ice breakup: A neglected factor in river ecology, *Can. J. Civ. Eng.*, *30*, 128–144.

Prowse, T. D., B. Bonsal, C. R. Duguy, D. O. Hessen, and V. S. Vuglinsky (2007), River and lake ice, in *Global Outlook for Ice and Snow*, pp. 201–214, U. N. Environ. Programme, Nairobi.

Romeiser, R., H. Runge, S. Suchandt, J. Sprenger, H. Weilbeer, A. Sohrmann, and D. Stammer (2007), Current measurements in rivers by spaceborne along-track InSAR, *IEEE Trans. Geosci. Remote Sens.*, *45*(12), 4019–4031.

Romeiser, R., S. Suchandt, H. Runge, U. Steinbrecher, and S. Grünler (2010), First analysis of TerraSAR-X along-track InSAR-derived current fields, *IEEE Trans. Geosci. Remote Sens.*, *48*(2), 820–829.

Shiklomanov, A. I., T. I. Yakovleva, R. B. Lammers, I. P. Karasev, C. J. Vörösmarty, and E. Linder (2006), Cold region river discharge uncertainty—Estimates from large Russian rivers, *J. Hydrol.*, *326*, 231–256.

Siegmund, R., M. Q. Bao, S. Lehner, and R. Mayerle (2004), First demonstration of surface currents imaged by hybrid along- and cross-track interferometric SAR, *IEEE Trans. Geosci. Remote Sens.*, *42*(3), 511–519.

Smith, L. C. (2002), Emerging applications of interferometric synthetic aperture radar (InSAR) in geomorphology and hydrology, *Ann. Assoc. Am. Geogr.*, *92*(3), 385–398.

Unterschultz, K. D., J. van der Sanden, and F. E. Hicks (2009), Potential of RADARSAT-1 for the monitoring of river ice: Results of a case study on the Athabasca River at Fort McMurray, Canada, *Cold Reg. Sci. Technol.*, *55*(2), 238–248.

Vincent, F., D. Raucoules, T. Degroeve, G. Edwards, and M. A. Mostafavi (2004), Detection of river/sea ice deformation using satellite interferometry: Limits and potential, *Int. J. Remote Sens.*, *25*(18), 3555–3571.

White, K. D., and S. Beltaos (2008), Development of ice-affected stage-frequency curves, in *River Ice Breakup*, edited by S. Beltaos, pp. 305–348, Water Resour., Highlands Ranch, Colo.

A. Kääb, Department of Geosciences, University of Oslo, PO Box 1047 Blindern, N-0316 Oslo, Norway. (kaeaeb@geo.uio.no)

T. Prowse, Division of Hydrologic Water and Climate Impacts Research Centre, Environment Canada, University of Victoria, PO Box 3060 STN CSC, Victoria, BC V8W 3R4, Canada. (prowset@uvic.ca)